Structure-stability relationships for all-silica structures

K. de Boer, A. P. J. Jansen, and R. A. van Santen
Laboratory for Inorganic Chemistry and Catalysis, Eindhoven University of Technology, P.O. Box 513, 5600 MB Eindhoven, The Netherlands
(Received 27 March 1995)

We will discuss predictions for the stability and structures of all-silica zeolitic structures. We will show that we have derived a shell-model potential, based on *ab initio* calculations, which gives good predictions for the structure and stability of all-silica structures. We will compare three shell-model predictions with two rigid-ion model predictions for the structure and stability of silicates. We will show that shell-model predictions for the relative stability of zeolites are much closer to experiment than rigid-ion model predictions, due to the canceling of covalent and electrostatic terms in the shell models which does not occur in the rigid-ion models. Using the potentials with the highest predictive power on both stabilities and structures of silicates we will discuss structure-stability relationships that have been proposed in the literature.

I. INTRODUCTION

The synthesis of high silica zeolites is important for catalysis because of their thermal, hydrothermal and acidic stabilities, good resistance to aging, and in particular hydrophobicity which favors the reaction with organic molecules.[1] Despite the new high and pure-silica zeolites that have been reported,[2] the relation between crystal structure and thermodynamics is still poorly understood. Insight into the factors that govern the relative stability of silica zeolites is important for their synthesis which is still a difficult process.[2] Modeling provides a powerful tool for gaining that insight for several reasons. Many more silica zeolites, than have been synthesized yet, can be modeled so that experimentally observed relations between structure and stability can be tested more thoroughly.[3–8] The calculated data and the structure are consistent, whereas sometimes in literature[9] measured enthalpies on alumina-free samples are correlated with structural data on samples which contain Al, due to the lack of structure data on pure-silica samples. Furthermore, only for a few systems there exists single-crystal data and other structural data are obtained from x-ray powder diffraction data which is considered less reliable.[9] Given a good potential, structures can be predicted which are even more accurate than the x-ray powder data (Ref. 10, and this work).

In this paper we will discuss predictions for the stabilities and structures for pure-silica zeolites. Our first aim is to make an extensive comparison between our recently developed shell-model potentials,[11,12] denoted as the BJS I (Boer-Jansen-van Santen) and BJS II potentials, with the shell-model potential of Catlow *et al.*[7] denoted as the Jackson-Catlow (JC) potential, and the rigid-ion model potentials of Kramer *et al.*[13] and Tsuneyuki *et al.*,[14] respectively, denoted as the Kramer-Farragher-van Beest-van Santen (KFBS) and Tsuneyuki-Tsukada-Aoki (TTA) potentials. First we will show that we have derived a new shell-model potential mainly based on *ab initio* data which gives very accurate structure predictions and reasonable predictions for the stability of zeolites. Furthermore, we will show that the BJS I, BJS II, and JC shell-model predictions for the stability of zeolites are closer to experiment than the rigid-ion model predictions. We also show that this is caused by the partial canceling of covalent and electrostatic energy terms in the shell model which does not occur in the rigid-ion models. Furthermore, we will use the BJS II and JC potential for the exploration of hypothetical structures and structure-stability relationships. Those potentials predict, contrary to other modeling studies,[8,15] that there is no direct correlation between the density and the relative stability of silica polymorphs, which agrees with recent measurements. The potentials also predict that stabilization of low-density silicates must be caused by small Si-O-Si bond angles in those systems, which supports the work of Petrovic *et al.*[9] Our results further show that, a *linear* relationship between the destabilization and the percentage of angles smaller than or equal to 140° in the structure, as also suggested by Petrovic *et al.*,[9] does not exist for a large number of structures.

II. COMPUTATIONAL DETAILS

A. Structures

We have studied the following structures which exist in pure or high-silica form: α-quartz,[16] coesite,[17] ZSM-12,[20] ZSM-18,[21] cubic faujasite,[22] monoclinic ZSM-5,[23] SSZ-24,[24] and ZSM-22,[25] which include the structures for which the enthalpies have been measured recently.[9] In order to study structure-stability relations more thoroughly we have also considered some hypothetical structures in the low-density region which were derived from the original structures by replacing Al, B, Be, or Zn by Si and deleting the compensations cations or water. The original structures are thomsonite,[26] chabazite,[27] lovdarite,[28] VPI-7,[29] and hexagonal faujasie.[30] The remaining zeolitic structures studied, have been synthesized with varying Al/Si ratio and are treated as purely siliceous. Those are mentioned in the references cited in Table V. The structures are calculated using THBREL using the above structures as starting structures.

B. Calculations

The minimizations are performed by the THBREL code[33] which is based on lattice dynamics[34] and the use of inter-

atomic potentials. The electrostatic interactions are calculated using an Ewald summation. No symmetry constraints are applied during the minimization. THBREL also generates the elastic constant tensor (elastic stiffness tensor) and the high- and low-frequency dielectric tensor. Using the relaxed structure and the interatomic potential, we have also calculated phonon spectra close to the Γ point with the THBPHON code,[35] which serves as a check on the stability of the structures.[10] Furthermore we decomposed for all potentials the predicted lattice energy per SiO_2 unit, relative to that of α quartz, into covalent and electrostatic contributions. This decomposition is obtained by calculating the energies of the relaxed structures with only the relevant interactions turned on.

C. Interatomic potentials

We have employed two rigid-ion model potentials derived by Kramer *et al.*[13] and Tsuneyuki *et al.*,[14] respectively, denoted as the KFBS and TTA potential. We have used the shell-model potential of Catlow *et al.*,[7] denoted as the JC potential, and the two recently developed shell-model potentials of de Boer *et al.*, denoted as the BJS I (Ref. 11) and BJS II potentials. The BJS I and BJS II potentials have the following form:

$$E^{\text{pot}}=\sum_{\substack{i,j\\ i<j}}\left[A_{ij}\exp\left(\frac{-r_{ij}}{\rho_{ij}}\right)-\frac{C_{ij}}{r_{ij}^6}\right]+um_{i<j}^{i,j}\frac{q_iq_j}{r_{ij}}\sum_{\substack{i,j\\ i<j}}\frac{q_iq_j}{r_{ij}}+\frac{1}{2}\sum_i k(r_{i,\text{shell}}-r_{i,\text{core}})^2. \quad (1)$$

The first and second terms in relation (1) constitute the well-known Buckingham form, which describes the covalent interactions between all atoms. The O-O interaction in this term only acts through the shells, the Si-O interaction acts between the O shell and the Si ion. Only the O atom is described as a core and a shell. The Si atom has no shell, only a core. The third term is the Coulomb interaction which describes all electrostatic interactions between cores, between shells, and between cores and shells belonging to different atoms. The fourth term is the harmonic interaction, which acts between core and shell of the same O atom.

The Buckingham parameters of the BJS I potential are derived from fitting on *ab initio* potential-energy surfaces of the $Si(OH)_4$ cluster. The shell and atomic charges are obtained from, respectively, *ab initio* polarizabilities and dipoles of $(HO)_3SiOSi(OH)_3$ clusters. The fit procedures are done iteratively so that the parameter sets fits self-consistently all *ab initio* data employed. A derivation of this *ab initio* shell-model potential is given in Ref. 11.

The BJS II potential is an adaptation of the BJS I potential. The Buckingham parameters of the BJS II potential are derived as described for the BJS I potential. The shell and atomic charges are fitted such that the best structure of α quartz is obtained, which was necessary to remedy the too small Si-O-Si bond angle in α quartz as predicted by the BJS I potential (Ref. 11, and also this work). The fitting of the electrostatic and Buckingham parameters is done iteratively to yield a parameter set which fits all data self-consistently.

TABLE I. Parameters of the BJS I and BJS II potentials. Charges in the BJS I potential: $q_{Si}=2.7226$, $q_{O_s}=-2.0125$, $q_{O_c}=0.6512$. Charges in the BJS II potential: $q_{Si}=3.0906$, $q_{O_s}=-2.0948$, $q_{O_c}=0.5495$. For both potentials $C=0$. The subscripts c and s denote, respectively, core and shell.

Interaction	A (eV)	ρ (Å)	k (eV Å^{-2})
BJS I			
O_s-O_s	266 757.0	0.173 411	
Si-O_s	18 122.0	0.170 77	
O_c-O_s			34.98
BJS II			
O_s-O_s	4 591 190.0	0.139 636	
Si-O_s	5 086.63	0.212 366	
O_c-O_s			33.52

This potential is treated in more detail elsewhere.[12] Parameters of the BJS I and BJS II potentials are shown in Table I.

The cutoffs applied in the THBREL and THBPHON calculations for the TTA, KFBS, and JC potentials are 10 Å.[5,14] The covalent OO interactions of the BJS I and BJS II potentials are applied with a cutoff of 3.5 Å, because for larger distances all covalent potential terms are effectively zero. The covalent SiO interaction of the latter potentials is applied with a cutoff of 2.5 Å (i.e., in between the nearest and next-nearest Si and O neighbors) to simulate a real Si-O bond.

III. RESULTS

We will first discuss predictions of structures, followed by an evaluation of predicted energies. Using the potentials which predict those quantities most accurate, we will subsequently discuss structure-stability relationships that have been proposed in literature.

A. Structures

1. Pure silica structures

Table II shows that in the case of α quartz, cubic faujasite, SSZ-24, ZSM-18, ZSM-22, and monoclinic ZSM-5, the BJS II and JC predictions are equally accurate and much closer to experiment than the other predictions. This table also shows that the adaptation of the BJS II potential to correct the Si-O-Si bond angle in α quartz also works for many other structures. Both the BJS II and JC potentials predict Si-O-Si bond angles which are slightly too small. The KFBS and TTA potentials predict too large Si-O-Si bond angles and the latter also predicts too large Si-O distances. For SSZ-24 both the KFBS and TTA potentials predict the same structure consisting of layers which is not in accordance with experiment. This has been shown previously in detail for the KFBS potential.[37] For ZSM-5, the TTA and KFBS potentials predict the high-temperature orthorhombic phase as the most stable form. This is not in agreement with the experimental fact that the low-temperature monoclinic phase is the most stable.[23] Thus the TTA and KFBS potentials show similar behavior. For coesite the BJS I and KFBS potentials perform the best, which is consistent with their good performance on α quartz subjected to high pressures, which has been shown and ac-

TABLE II. Predictions for all-silica structures, compared with experiment. Distances are in Å and angles in degrees. References denote experiment. FAU denotes cubic faujasite. ZSM-5-m denotes monoclinic ZSM-5.

Property	Expt.	BJS I	BJS II	KFBS	JC	TTA
α quartz (Ref. 16)						
a	4.902	4.751	4.854	4.941	4.836	5.018
c	5.400	5.213	5.339	5.449	5.347	5.548
γ	120.0	120.0	120.0	120.0	120.0	120.0
$d_{\text{Si-O}_s}$	1.612	1.621	1.606	1.597	1.608	1.630
$d_{\text{Si-O}_l}$	1.613	1.624	1.608	1.605	1.615	1.642
$\langle d_{\text{Si-O}} \rangle$	1.613	1.623	1.607	1.601	1.611	1.636
$\langle \angle_{\text{Si-O-Si}} \rangle$	142.4	131.7	140.1	148.5	139.1	146.8
$\angle_{\text{O-Si-O}_s}$	108.6	104.6	106.6	107.9	108.3	107.5
$\angle_{\text{O-Si-O}_l}$	110.7	112.9	111.9	115.0	111.3	115.7
Symmetry	$P3_121$	$P3_121$	$P3_121$	$P3_121$	$P3_121$	$P3_121$
Coesite (Ref. 17)						
a	7.137	6.832	6.776	7.138	6.806	7.256
b	12.37	12.14	12.36	12.49	12.29	12.76
c	7.174	7.019	7.086	7.271	7.115	7.434
γ	120.3	120.04	121.72	120.76	119.42	121.07
$d_{\text{Si-O}_s}$	1.595	1.566	1.559	1.579	1.569	1.608
$d_{\text{Si-O}_l}$	1.621	1.637	1.635	1.620	1.628	1.657
$\langle d_{\text{Si-O}} \rangle$	1.609	1.614	1.609	1.604	1.611	1.638
$\angle_{\text{Si-O-Si}_s}$	137.2	126.5	127.9	144.7	132.6	143.9
$\angle_{\text{Si-O-Si}_l}$	180.0	180.0	180.0	180.0	180.0	180.0
$\langle \angle_{\text{Si-O-Si}} \rangle$	150.8	139.9	142.1	154.4	143.8	153.96
$\angle_{\text{O-Si-O}_s}$	108.0	104.6	103.5	104.3	104.85	104.0
$\angle_{\text{O-Si-O}_l}$	110.4	114.7	114.1	115.7	112.7	116.4
Symmetry	$C2/c$	$C2/c$	$C2/c$	$C2/c$	$C2/c$	$C2/c$
Stishovite (Ref. 18)						
a	4.177	4.089	4.029	4.149	4.025	4.264
c	2.665	2.591	2.638	2.662	2.775	2.747
u	0.306	0.307	0.296	0.305	0.304	0.304
$d_{\text{Si-O}_s}$	1.757	1.751	1.757	1.755	1.782	1.810
$d_{\text{Si-O}_l}$	1.809	1.715	1.689	1.790	1.728	1.836
$\langle d_{\text{Si-O}} \rangle$	1.774	1.738	1.734	1.764	1.764	1.818
$\angle_{\text{Si-O-Si}}$	130.7	132.2	131.3	130.7	128.8	130.7
$\angle_{\text{O-Si-O}_1}$	81.3	84.5	82.7	81.3	77.7	81.30
$\angle_{\text{O-Si-O}_2}$	180.0	180.0	180.0	180.0	180.0	180.0
$\angle_{\text{O-Si-O}_3}$	90.0	90.0	90.0	90.0	90.0	90.0
$\angle_{\text{O-Si-O}_4}$	98.7	95.5	97.3	98.7	102.3	98.7
Symmetry	$P4_2/mnm$	$P4_2/mnm$	$P4_2/mnm$	$P4_2/mnm$	$P4_2/mnm$	$P4_2/mnm$
FAU (Ref. 22)						
a	24.26	23.87	24.11	24.78	24.23	25.39
α	90.00	90.0	90.0	90.0	90.0	90.0
$d_{\text{Si-O}_s}$	1.597	1.608	1.591	1.600	1.599	1.636
$d_{\text{Si-O}_l}$	1.616	1.62	1.616	1.620	1.614	1.658
$\langle d_{\text{Si-O}} \rangle$	1.606	1.616	1.604	1.609	1.607	1.646
$\angle_{\text{Si-O-Si}_s}$	138.4	133.5	135.6	143.3	137.6	143.9
$\angle_{\text{Si-O-Si}_l}$	149.4	139.8	150.0	160.4	148.9	161.7
$\langle \angle_{\text{Si-O-Si}} \rangle$	143.7	136.4	142.6	152.7	143.3	153.7
$\angle_{\text{O-Si-O}_s}$	108.0	102.4	106.2	104.8	107.5	104.4
$\angle_{\text{O-Si-O}_l}$	111.5	114.4	112.4	116.0	112.0	116.8
Symmetry	$Fd\bar{3}m$	$Fd\bar{3}m$	$Fd\bar{3}m$	$Fd\bar{3}m$	$Fd\bar{3}m$	$Fd\bar{3}m$

TABLE II. (*Continued*).

Property	Expt.	BJS I	BJS II	KFBS	JC	TTA
SSZ-24 (Ref. 24)						
a	13.62	13.28	13.59	13.93	13.60	13.77
b	13.62	13.28	13.59	13.93	13.60	14.26
c	8.323	8.07	8.32	8.19	8.31	8.348
α	90.0	90.0	90.0	90.19	90.0	89.86
β	90.0	90.00	90.00	89.66	90.00	90.00
γ	120.0	120.0	120.0	122.1	120.0	118.9
$d_{\text{Si-O}_s}$	1.570	1.609	1.579	1.590	1.595	1.624
$d_{\text{Si-O}_l}$	1.619	1.622	1.601	1.623	1.608	1.660
$\langle d_{\text{Si-O}} \rangle$	1.596	1.615	1.593	1.605	1.602	1.641
$\angle_{\text{Si-O-Si}_s}$	142.2	134.5	144.3	140.8	144.5	140.3
$\angle_{\text{Si-O-Si}_l}$	164.7	140.4	161.3	179.86	154.7	179.5
$\langle \angle_{\text{Si-O-Si}} \rangle$	151.3	136.3	150.1	157.5	147.7	158.0
$\angle_{\text{O-Si-O}_s}$	96.99	105.6	105.9	104.3	107.8	103.9
$\angle_{\text{O-Si-O}_l}$	119.3	115.0	112.6	115.6	111.3	114.8
Symmetry	$P6/mcc$	$P6/m$	$P6/m$	$C2/c$	$P6/m$	$C2/c$
ZSM-11 (Ref. 19)						
a	20.07	19.39	19.93	20.47	19.95	20.92
b	20.07	19.66	19.93	20.47	19.95	20.92
c	13.41	13.02	13.34	13.73	14.05	14.04
α	90.0	90.0	90.0	90.0	90.0	90.0
$d_{\text{Si-O}_s}$	1.489	1.540	1.569	1.582	1.580	1.621
$d_{\text{Si-O}_l}$	1.686	1.721	1.602	1.628	1.614	1.665
$\langle d_{\text{Si-O}} \rangle$	1.597	1.611	1.591	1.607	1.600	1.643
$\angle_{\text{Si-O-Si}_s}$	144.1	129.2	142.8	150.3	141.7	150.8
$\angle_{\text{Si-O-Si}_l}$	165.3	172.1	169.0	175.9	163.7	175.9
$\langle \angle_{\text{Si-O-Si}} \rangle$	153.3	140.0	151.4	161.6	149.2	162.3
$\angle_{\text{O-Si-O}_s}$	99.7	99.3	104.2	105.9	103.7	104.6
$\angle_{\text{O-Si-O}_l}$	122.9	119.5	113.3	115.8	113.9	116.2
Symmetry	$I\bar{4}m2$	$P1$	$I\bar{4}$	$I\bar{4}m2$	$I\bar{4}$	$I\bar{4}m2$
ZSM-12 (Ref. 20)						
a	24.86	24.21	24.95	25.15	24.94	25.80
b	5.012	4.839	5.036	4.937	4.998	5.048
c	24.32	23.63	24.23	23.91	24.16	24.39
β	107.7	107.2	107.6	106.5	107.37	106.8
$d_{\text{Si-O}_s}$	1.526	1.600	1.585	1.596	1.597	1.628
$d_{\text{Si-O}_l}$	1.698	1.625	1.609	1.622	1.610	1.663
$\langle d_{\text{Si-O}} \rangle$	1.596	1.615	1.593	1.605	1.602	1.641
$\angle_{\text{Si-O-Si}_s}$	134.3	129.2	136.9	137.9	137.7	137.2
$\angle_{\text{Si-O-Si}_l}$	158.6	149.9	159.2	167.8	157.3	168.6
$\langle \angle_{\text{Si-O-Si}} \rangle$	150.3	136.5	149.8	151.4	146.9	151.8
$\angle_{\text{O-Si-O}_s}$	103.3	104.1	105.5	105.1	106.1	104.4
$\angle_{\text{O-Si-O}_l}$	114.2	116.6	113.2	117.5	113.2	118.4
Symmetry	$C2/c$	$C2/c$	$C2/c$	$C2/c$	$C2/c$	$C2/c$
ZSM-18 (Ref. 21)						
a	13.18	12.86	12.97	13.30	13.04	13.63
c	15.85	15.27	15.49	15.95	15.59	16.33
γ	120.0	120.0	120.0	120.0	120.0	120.0
$d_{\text{Si-O}_s}$	1.577	1.569	1.570	1.589	1.588	1.623
$d_{\text{Si-O}_l}$	1.631	1.643	1.638	1.628	1.628	1.668
$\langle d_{\text{Si-O}} \rangle$	1.613	1.615	1.604	1.609	1.606	1.645
$\angle_{\text{Si-O-Si}_s}$	134.7	125.8	128.5	139.3	131.7	139.8
$\angle_{\text{Si-O-Si}_l}$	180.00	180.0	180.0	180.00	180.0	180.0
$\langle \angle_{\text{Si-O-Si}} \rangle$	147.4	137.6	143.8	153.4	144.8	154.2
$\angle_{\text{O-Si-O}_s}$	105.3	103.5	105.7	100.7	106.6	100.1
$\angle_{\text{O-Si-O}_l}$	111.98	114.3	113.4	116.4	112.5	117.1
Symmetry	$P6_3/m$	$P6_3/m$	$P6_3/m$	$P6_3/m$	$P6_3/m$	$P6_3/m$

TABLE II. (*Continued*).

Property	Expt.	BJS I	BJS II	KFBS	JC	TTA
ZSM-22 (Ref. 25)						
a	13.89	13.41	13.81	13.96	13.87	14.33
b	17.42	17.04	17.37	17.63	17.41	18.14
c	5.03	4.89	5.032	5.094	5.005	5.261
γ	90.0	90.0	90.0	90.0	90.0	90.0
$d_{\text{Si-O}_s}$	1.567	1.583	1.586	1.596	1.592	1.630
$d_{\text{Si-O}_t}$	1.627	1.629	1.597	1.617	1.609	1.656
$\langle d_{\text{Si-O}} \rangle$	1.600	1.611	1.591	1.604	1.599	1.640
$\angle_{\text{Si-O-Si}_s}$	141.03	127.5	145.70	146.8	143.1	151.2
$\angle_{\text{Si-O-Si}_t}$	156.6	158.3	155.6	162.0	153.9	163.4
$\langle \angle_{\text{Si-O-Si}} \rangle$	151.3	139.3	151.4	156.3	150.0	158.9
$\angle_{\text{O-Si-O}_s}$	107.6	103.5	105.3	106.2	106.2	106.0
$\angle_{\text{O-Si-O}_t}$	111.2	115.6	113.0	114.5	112.8	114.9
Symmetry	$Cmc2_1$	$P2_1$	$Cmc2_1$	$Cmc2_1$	$Cmc2_1$	$Cmc2_1$
ZSM-5-m (Ref. 23)						
a	20.10	19.57	19.97	20.38	19.98	20.89
b	19.88	19.27	19.75	20.34	19.74	20.82
c	13.37	13.03	13.20	13.68	13.32	14.01
α	90.44	90.8	90.36	90.0	90.53	90.0
$d_{\text{Si-O}_s}$	1.583	1.589	1.580	1.594	1.591	1.629
$d_{\text{Si-O}_t}$	1.608	1.631	1.603	1.622	1.613	1.662
$\langle d_{\text{Si-O}} \rangle$	1.595	1.611	1.592	1.606	1.601	1.642
$\angle_{\text{Si-O-Si}_s}$	141.2	128.5	139.6	149.9	138.8	151.3
$\angle_{\text{Si-O-Si}_t}$	169.0	155.4	170.5	177.6	166.5	177.3
$\langle \angle_{\text{Si-O-Si}} \rangle$	153.9	130.0	151.0	162.1	148.8	163.0
$\angle_{\text{O-Si-O}_s}$	107.10	99.73	103.9	105.3	104.5	104.9
$\angle_{\text{O-Si-O}_t}$	111.63	117.0	113.4	114.9	112.72	115.5
Symmetry	$P2_1/c$	$P2_1/c$	$P2_1/c$	$Pnma$ [a]	$P2_1/c$	$Pnma$ [a]

[a]The TTA and KFBS potentials predict orthorhombic ZSM-5 as the most stable form, when both the orthorhombic and monoclinic structure are used as a starting structure.

counted for elsewhere.[36] We notice that coesite has been reported with space group $P121/A1$ with no Si-O-Si bond angles of 180° (Refs. 38 and 39) and as a structure containing Si-O-Si bond angles of 180°, and spacegroup $C2/c$.[17] All potentials predict essentially the latter structure. Also the high-pressure structure stishovite is the most accurately predicted by the KFBS and BJS I potentials. See Table II. The BJS II potential predicts the long Si-O distances in stishovite too short. The JC potential predicts, besides less accurate Si-O distance, a too large distortion of the O-Si-O angles. These results will further discussed in the section *calculated energies versus experiment.*

The results on ZSM-11 and ZSM-12 show that the JC and BJS II predictions of unit-cell parameters are equally accurate and closest to the experiment. However, the predicted smallest and largest Si-O distances are, respectively, much longer and shorter than the experimental values. The predicted range of O-Si-O angles for ZSM-11 is much smaller than in the experiment. The BJS II and JC predictions might, however, be closer to the actual values than the experimental data reported so far, for the following reasons: Petrovic *et al.*[9] already noticed that the experimental data for the O-Si-O angles and the Si-O distances reported on ZSM-11 and ZSM-12 deviate much from those normally encountered in most reliable single-crystal studies on silicates and that it remains to be seen if those experimental data can be confirmed by further experiments.[9] Furthermore, if ZSM-11 and ZSM-12 would really contain those deviating distances and angles, the one would expect that only the JC potential, which is derived from structure data on α quartz, would disagree with experiment. However *both* the JC and the almost *ab initio* BJS II potentials predicted almost the same values which only deviate from experiment for these angles and distances. Furthermore, we have shown that the BJS II and JC potentials give very accurate predictions for well-defined structures like α quartz, cubic faujasite, and monoclinic ZSM-5 for which structure data is obtained from single-crystal measurements. Thus the BJS II and JC predictions indicate that the measured O-Si-O angles and Si-O distances in ZSM-11 and ZSM-12 might not be accurate. We conclude that the BJS II and JC potentials are the most accurate on predictions for silicate structures with a density lower or equal to that of α quartz.

2. *Hypothetical all-silica structures*

The results on the hypothetical structure calculations are shown in Table III. The hexagonal faujasite and chabazite results show that both the BJS II and JC potentials predict

TABLE III. Predictions for hypothetical all-silica structures compared with experimental original structures. Symbols and units are the same as in Table II, EMT denotes hexagonal faujasite, THO denotes thomsonite, CHA denotes chabazite. References denote experiment.

	Expt.	BJS I	BJS II	KFBS	JC	TTA
EMT (Ref. 30)						
a	17.42	16.89	17.05	17.53	17.13	17.95
c	28.42	27.53	27.83	28.62	27.98	29.31
γ	120.0	120.00	120.0	120.0	120.0	120.0
$d_{\text{Si-O}_s}$	1.630	1.607	1.591	1.600	1.599	1.635
$d_{\text{Si-O}_l}$	1.631	1.621	1.616	1.621	1.615	1.659
$\langle d_{\text{Si-O}} \rangle$	1.631	1.616	1.604	1.609	1.607	1.646
$\angle_{\text{Si-O-Si}_s}$	141.5	133.3	135.5	143.3	137.5	143.9
$\angle_{\text{Si-O-Si}_l}$	145.8	140.3	150.4	161.0	149.4	162.0
$\langle \angle_{\text{Si-O-Si}} \rangle$	142.9	136.5	142.8	152.9	143.47	153.8
$\angle_{\text{O-Si-O}_s}$	109.4	102.3	106.1	104.7	107.2	104.4
$\angle_{\text{O-Si-O}_l}$	109.5	114.4	112.5	116.2	112.0	116.9
Symmetry	$P6_3/mmc$	$P6_3/mmc$	$P6_3/mmc$	$P6_3/mmc$	$P6_3/mmc$	$P6_3/mmc$
THO (Ref. 26)						
a	13.23 (13.85)	13.52	13.65	13.98	13.75	14.32
b	13.08 (6.92)	6.762	6.827	6.99	6.876	7.161
c	13.05 (6.43)	6.224	6.315	6.47	6.357	6.625
α	90.0 (90.0)	90.0	90.0	90.0	90.0	90.0
$d_{\text{Si-O}_s}$	1.614 (1.569)	1.565	1.562	1.585	1.578	1.619
$d_{\text{Si-O}_l}$	1.755 (1.632)	1.629	1.617	1.620	1.615	1.659
$\langle d_{\text{Si-O}} \rangle$	1.681 (1.614)	1.613	1.602	1.609	1.605	1.646
$\angle_{\text{Si-O-Si}_s}$	126.9 (142.0)	131.7	138.3	148.2	140.46	148.9
$\angle_{\text{Si-O-Si}_l}$	140.9 (180.0)	180.0	180.0	180.0	179.99	180.0
$\langle \angle_{\text{Si-O-Si}} \rangle$	135.5 (150.8)	142.0	147.9	155.6	149.4	156.2
$\angle_{\text{O-Si-O}_s}$	101.5 (108.0)	106.2	107.4	103.1	108.1	102.6
$\angle_{\text{O-Si-O}_l}$	113.7 (111.1)	116.2	113.8	113.6	112.2	113.9
Symmetry	$Pncn$ ($Pmma$)	$P2/c$	$Pmma$	$Pmma$	$Pmma$	$Pmma$
CHA (Ref. 27)						
a	9.441	9.102	9.144	9.398	9.198	9.620
α	93.09	94.77	94.66	94.91	94.75	94.95
$d_{\text{Si-O}_s}$	1.616	1.601	1.593	1.599	1.599	1.635
$d_{\text{Si-O}_l}$	1.683	1.609	1.603	1.619	1.607	1.657
$\langle d_{\text{Si-O}} \rangle$	1.642	1.605	1.599	1.609	1.603	1.645
$\angle_{\text{Si-O-Si}_s}$	140.35	140.0	142.2	153.7	144.2	154.5
$\angle_{\text{Si-O-Si}_l}$	157.66	144.4	147.3	155.7	148.7	156.5
$\langle \angle_{\text{Si-O-Si}} \rangle$	148.1	142.6	145.7	154.9	147.0	155.4
$\angle_{\text{O-Si-O}_s}$	98.57	104.1	106.7	105.1	107.6	104.7
$\angle_{\text{O-Si-O}_l}$	113.3	114.0	112.4	114.7	111.7	115.2
Symmetry	$R\bar{3}m$	$R\bar{3}m$	$R\bar{3}m$	$R\bar{3}m$	$R\bar{3}m$	$R\bar{3}m$
Lovdarite (Ref. 28)						
a	39.58	40.0	41.13		41.13	
b	6.931	6.979	7.076		7.107	
c	7.152	6.995	7.076		7.115	
α	90.0	90.0	90.0		90.0	
$d_{\text{Si-O}_s}$	1.560	1.596	1.581		1.630	
$d_{\text{Si-O}_l}$	1.699	1.643	1.639		1.594	
$\langle d_{\text{Si-O}} \rangle$	1.622	1.618	1.607		1.608	
$\angle_{\text{Si-O-Si}_s}$	122.1	124.6	128.1		140.0	
$\angle_{\text{Si-O-Si}_l}$	162.9	148.2	166.3		159.8	
$\langle \angle_{\text{Si-O-Si}} \rangle$	137.5	135.9	142.9		143.4	
$\angle_{\text{O-Si-O}_s}$	102.5	103.4	107.3		107.6	
$\angle_{\text{O-Si-O}_l}$	116.6	115.2	114.5		112.4	
Symmetry	$Pma2$	$Pma2$	$P4_2/mmc$		$Pma2$	

TABLE III. (*Continued*).

	Expt.	BJS I	BJS II	KFBS	JC	TTA
VPI-7 (Ref. 29)						
a	40.62	39.79	41.12		40.98	
b	7.179	6.945	7.053		7.079	
c	7.179	6.945	7.053		7.079	
α	90.0	89.7	90.0		89.9	
$d_{\text{Si-O}_s}$	1.569	1.592	1.581		1.593	
$d_{\text{Si-O}_l}$	1.657	1.642	1.636		1.630	
$\langle d_{\text{Si-O}} \rangle$	1.605	1.620	1.607		1.610	
$\angle_{\text{Si-O-Si}_s}$	132.8	124.9	128.0		131.0	
$\angle_{\text{Si-O-Si}_l}$	170.8	148.3	163.7		153.8	
$\langle \angle_{\text{Si-O-Si}} \rangle$	145.6	135.0	142.4		142.4	
$\angle_{\text{O-Si-O}_s}$	104.0	103.8	106.8		106.5	
$\angle_{\text{O-Si-O}_l}$	115.7	116.0	114.4		113.5	
Symmetry	$I\bar{4}m2$	$Fdd2$	$Fdd2$		$Fdd2$	

smaller unit cells then the experiment which is mainly due to the predicted smaller T-O distances, which are smaller in all-silica structures than in Al containing samples, consistent with experimental findings.[45] (We use T instead of Si when in the experiment Si might have been replaced by Al or another atom.) The KFBS and TTA potentials predict for the hypothetical structures, besides shorter T-O distances, larger T-O-T angles than the experiment. As those potentials also predict T-O-T angles which are too large for the pure silicates, as shown in Table II, this seems an artifact of the potentials, and not an effect of the substitution of Al by Si. Thomsonite (Si/Al 1:1) shows a spectacular effect on substitution of Al by Si. All potentials predict for this structure a decrease of the T-O distances and opening of the T-O-T angles. The largest T-O-T angle becomes 180° causing the structure to change its symmetry. Due to its higher symmetry the unit cell almost halves. We also notice that the JC and BJS II predictions for that structure are close to the one as proposed by Gnechten *et al.*[26] (data in parentheses).

Although KFBS predictions for the all-silica forms of lovdarite and VPI-7 have been reported before,[40] we could not obtain satisfactory KFBS and TTA predictions for those structures. The calculated structures did not converge or had imaginary frequencies. On restarting those structures many local minima structures were obtained. Some of the structures obtained showed anomalous angles and distances and all symmetry was lost. These results might indicate that those structures cannot exist in the pure-silica form or that the potentials cannot cope with the structure. We think the latter is the case because the starting structure, used in the calculations, contains very narrow T-O-T angles which could not be reproduced by both potentials. This must be due to the too stiff Si-O-Si bond angle prediction, as we have shown in Table I and for the KFBS potential also in detail elsewhere.[36] The BJS II and JC potentials predict for lovdarite and VPI-7 an all-silica structure with virtually unchanged T-O-T angles and again shortened T-O distances. Thus, except for thomsonite, the predictions show for the hypothetical structures that on substitution of the Al, Be, B, or Zn by Si the T-O distances shorten and the T-O-T angles, even the narrow angles, virtually do not change.

B. Energies

1. Calculated energies versus experiment

Table IV shows the lattice energy per SiO_2 unit in the silica polymorph relative to that in α quartz which equals the change in energy for the process SiO_2 (α quartz) $\rightarrow SiO_2$(silica polymorph) further on denoted as ΔU_{trans}.

TABLE IV. ΔU_{trans} predictions for silicates compared with data of Petrovic *et al.* (Ref. 9) and Johnson *et al.* (Ref. 44). Silicates measured by Johnson *et al.* (Ref. 44) are denoted by daggers. ZSM-5-m denotes monoclinic ZSM-5. FAU and EMT denote, respectively, cubic and hexagonal faujasite. ΔU_{trans} is in kJ/mol SiO_2.

Silicate	Expt.	BJS I	BJS II	KFBS	JC	TTA
ZSM-11	8.2	5.54	1.83	42.56	10.91	38.26
ZSM-12	8.7	3.59	0.96	32.41	8.04	30.32
ZSM-5-m	8.2	4.78	1.93	37.00	9.55	33.79
SSZ-24	7.2	4.37	2.04	36.48	10.68	33.94
EMT	10.5	6.97	7.08	64.48	19.94	59.16
FAU	13.6	6.79	6.95	64.34	19.71	59.24
α cristobalite†	2.84	2.07	−1.50	16.36	3.39	16.56
Coesite†	2.93	5.68	0.84	−13.83	2.05	−16.74
Stishovite†	51.88	40.99	−48.40	−15.56	131.56	5.69

The latter is compared with the experimental enthalpy change ΔH_{trans}, which equals ΔU_{trans} for solid-state reactions, as the ΔpV term is negligible. Temperature effects on ΔU_{trans} and ΔH_{trans} are also neglected, because free-energy minimizations on α quartz at $T=300$ K predicted for several potentials a negligible change in lattice energy of α quartz ranging from 0.5 to 0.001 kJ/mol. Free-energy minimizations are discussed elsewhere.[41] We do not expect this effect to be larger in other silicates because experiments[42,43] have shown that temperature-induced structural changes in other silicates are small and comparable to those in α quartz. We will thus compare 0-K calculations of ΔU_{trans} with the experimental ΔH_{trans} obtained at 300 K. Only the JC and BJS I potentials predict correctly that the dense silicates coesite and stishovite are more unstable than α quartz, as shown in Table IV. The BJS I potential gives a reasonable prediction of the structure (see Table II) and relative stability of stishovite, despite the fact that in this polymorph the silicon is sixfold-coordinated, while the parameters of this potential are derived from *ab initio* potential-energy surfaces of fourfold-coordinated clusters.[11] This is not so surprising as it may seem at first sight because in the calculation of those potential energy surfaces the Si-O bond length was stretched to 2.00 Å and the O-Si-O bond angle was lowered to 70°, well beyond those distances and angles in stishovite. The BJS II potential gives a worse prediction for both the structure and relative stability of stishovite. Table II shows that the less accurate BJS II prediction of the structure of stishovite is mainly due to too small predicted Si-O distances. As the remaining distances and angles are predicted accurately, these too short predicted Si-O distances might stabilize the predicted stishovite so much that it becomes more stable than α quartz, which is not in agreement with experiment. Although the BJS II potential is derived from the same potential-energy surfaces as the BJS I potential (Ref. 11, and this work), the less accurate BJS II prediction for stishovite might be due to the inclusion of data on the α-quartz structure in the parametrization of this potential. Although the latter has improved the BJS II predictions for a large range of structures, this potential is thus not suitable to model stishovite. Table IV shows that the JC prediction of the ΔU_{trans} for stishovite is predicted far too high. As some of the Si-O bond lengths are predicted too small and others too large (see Table II), this might be caused by the three-body bond-angle term in the potential which destabilizes O-Si-O angles deviating from the ideal tetrahedral value. KFBS and TTA results on stishovite are discussed in literature.[13] Furthermore, Table IV shows that the predictions of the BJS I, BJS II, and JC shell-model potentials are closer to experiment than the rigid-ion model predictions. To account for the results in Table IV we have decomposed the calculated ΔU_{trans} into covalent and electrostatic contributions.

2. *Decomposition of the calculated* ΔU_{trans}

Table V shows the silicates for which we have done ΔU_{trans} calculations. We have decomposed ΔU_{trans}, as predicted by the rigid-ion model potentials, into contributions

TABLE V. Predicted densities for the studied silicates. Densities are in number of T atoms per 1000 Å^3. ZSM-5-o denotes orthorhombic ZSM-5, for other abbreviations see previous tables. Dashes denote structures that did not converge. References denote experiment.

Silicate	BJS I	BJS II	KFBS	JC	TTA
EMT (Ref. 30)	14.11	13.71	12.61	13.50	11.73
FAU (Ref. 22)	14.11	13.71	12.61	13.51	11.74
ZSM-18 (Ref. 21)	15.55	15.05	13.91	14.82	12.95
Chabazite (Ref. 27)	16.09	15.86	14.63	15.59	13.64
Thomsonite (Ref. 26)	17.57	16.99	14.75	16.64	14.72
Gismondine (Ref. 26)	18.82	17.38	15.80	17.13	–
Lovdarite (Ref. 28)	18.42	17.48	–	17.31	–
VPI-7 (Ref. 29)	18.77	17.60	–	17.53	–
Sodalite (Ref. 31)	19.37	17.86	22.81	17.85	15.43
Mordenite (Ref. 32)	19.22	17.98	17.14	17.87	15.73
SSZ-24 (Ref. 24)	19.49	18.03	17.81	18.02	16.70
ZSM-11 (Ref. 19)	19.33	18.11	16.69	18.05	15.57
ZSM-5-o[a] (Ref. 23)	19.70	18.24	16.93	18.27	15.76
ZSM-5-m[a] (Ref. 23)	19.54	18.31	16.93	18.05	15.76
Laumontite (Ref. 26)	19.37	18.51	18.27	18.27	–
Brewsterite (Ref. 32)	19.69	18.67	18.42	18.42	16.23
ZSM-12 (Ref. 20)	21.18	19.31	19.48	19.48	18.40
ZSM-22 (Ref. 25)	21.50	19.87	19.85	19.85	17.55
Analcime (Ref. 26)	20.57	20.23	19.90	19.90	18.21
α cristobalite (Ref. 43)	25.21	22.67	23.09	23.09	23.80
α quartz (Ref. 16)	29.44	27.54	27.70	27.70	24.79
Coesite (Ref. 17)	31.75	32.27	30.86	30.86	27.13
Stishovite (Ref. 18)	46.17	46.67	44.47	44.47	40.03

[a]The TTA and KFBS potentials predict orthorhombic ZSM-5 as the most stable form, when both the orthorhombic and monoclinic structures are used as a starting structure.

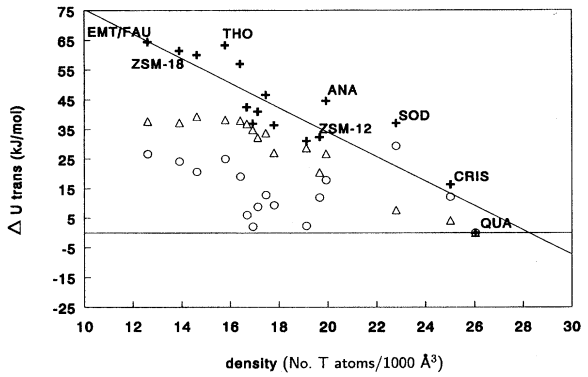

FIG. 1. Decomposition of ΔU_{trans} as predicted by the KFBS potential into $\Delta U_{\text{trans}}^{\text{els}}$ and $\Delta U_{\text{trans}}^{\text{cov}}$ for the silicates in Table V. Crosses depict ΔU_{trans}. Open circles depict $\Delta U_{\text{trans}}^{\text{els}}$ and open triangles depict $\Delta U_{\text{trans}}^{\text{cov}}$. The line represents a linear fit on ΔU_{trans} vs density.

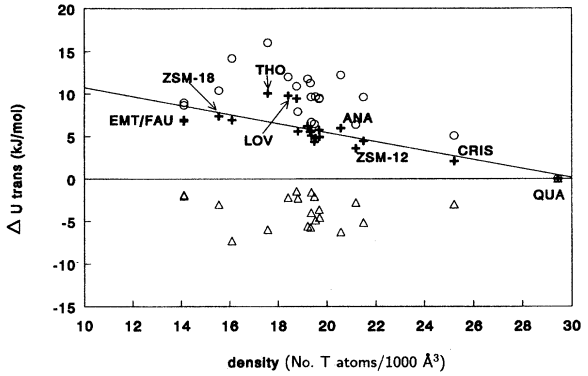

FIG. 3. Decomposition of ΔU_{trans} as predicted by the BJS I potential into $\Delta U_{\text{trans}}^{\text{els}}$ and $\Delta U_{\text{trans}}^{\text{cov}}$ for the silicates in Table V. Symbols are the same as in Fig. 1. The line represents a linear fit on ΔU_{trans} vs density.

due to the covalent interactions, denoted as $\Delta U_{\text{trans}}^{\text{cov}}$, and the term due to the point charges denoted as $\Delta U_{\text{trans}}^{\text{els}}$. The KFBS and TTA results on this decomposition are, respectively, shown in Figs. 1 and 2. Shell-model predictions for ΔU_{trans} are decomposed into a covalent term $\Delta U_{\text{trans}}^{\text{cov}}$, acting on the shells, without the intra-core-shell harmonic interaction, and an electrostatic term $\Delta U_{\text{trans}}^{\text{cov}}$ due to the atomic charges and the polarization, including the harmonic intra-core-shell interaction (see Figs. 3–5).

Figures 1 and 2 show that both rigid-ion models predict a positive $\Delta U_{\text{trans}}^{\text{cov}}$ and $\Delta U_{\text{trans}}^{\text{els}}$. We did not apply the energy correction of Kramer *et al.*[5] on the KFBS predictions. This correction was applied to the energy after the structure was optimized. As this makes the structure and the energy predictions inconsistent their conclusions seem hard to justify. $\Delta U_{\text{trans}}^{\text{els}}$ varies much more than $\Delta U_{\text{trans}}^{\text{cov}}$, thus the variation in ΔU_{trans} is mostly caused by the variation in $\Delta U_{\text{trans}}^{\text{els}}$. As shown in Figs. 3–5, the shell-model potentials predict that $\Delta U_{\text{trans}}^{\text{cov}}$ and $\Delta U_{\text{trans}}^{\text{els}}$ have opposite sign. The partial canceling of $\Delta U_{\text{trans}}^{\text{cov}}$ and $\Delta U_{\text{trans}}^{\text{els}}$ favors a less varying and smaller

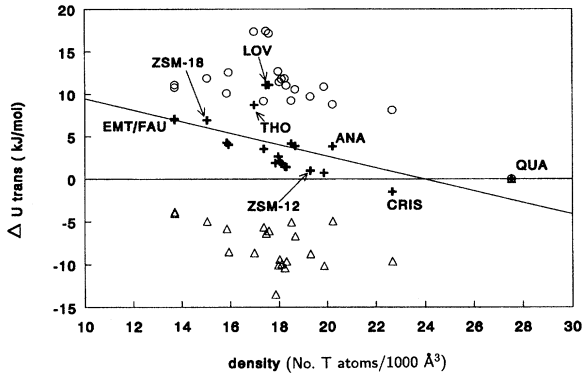

FIG. 4. Decomposition of ΔU_{trans} as predicted by the BJS II potential into $\Delta U_{\text{trans}}^{\text{els}}$ and $\Delta U_{\text{trans}}^{\text{cov}}$ for the silicates in Table V. Symbols are the same as in Fig. 1. The line represents a linear fit on ΔU_{trans} vs density.

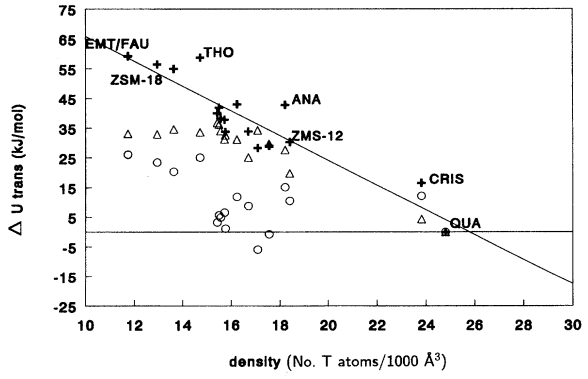

FIG. 2. Decomposition of ΔU_{trans} as predicted by the TTA potential into $\Delta U_{\text{trans}}^{\text{els}}$ and $\Delta U_{\text{trans}}^{\text{cov}}$ for the silicates in Table V. Symbols are the same as in Fig. 1. The line represents a linear fit on ΔU_{trans} vs density.

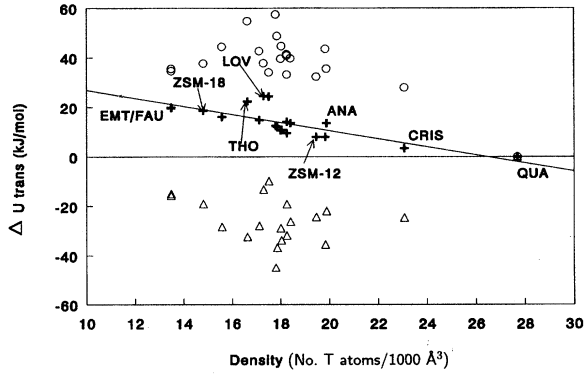

FIG. 5. Decomposition of ΔU_{trans} as predicted by the JC potential into $\Delta U_{\text{trans}}^{\text{els}}$ and $\Delta U_{\text{trans}}^{\text{cov}}$ for the silicates in Table V. Symbols are the same as in Fig. 1. The line represents a linear fit on ΔU_{trans} vs density.

ΔU_{trans} than in the rigid-ion model predictions.

All three shell-model potentials show a similar picture on their energy predictions, despite their different parameter sets. the two rigid-ion models potentials behave similar with respect to the energy predictions, irrespective of their different parameter sets. This implies that a good prediction of relative stabilities is not due to the use of a specific parameter set, as suggested in literature,[5] but due to the use of a shell-model potential.

C. Structure-stability relationships

In the previous section we have shown that the KFBS and TTA potentials do not give accurate predictions for both the structure and ΔU_{trans} of silicates. The BJS I potential gives reasonable predictions for the ΔU_{trans} but less accurate predictions for the structures of silicates. Both the JC and BJS II potentials give accurate structure predictions for a large range of silicates, whereas the JC potential also predicts accurately the ΔU_{trans} of the silicates mentioned in Table IV. Because the latter potentials predicts the silicate structures most accurately, we used them to investigate structure-stability relationships that have been proposed in literature.

1. Correlation between ΔU_{trans} and the density

The existence of a correlation between the density and ΔU_{trans} is subject to debate: Henson *et al.*[8] conclude on the basis of calculations with the JC potential that there is a correlation between ΔU_{trans} and the density. The latter was also concluded by de Vos *et al.* on the basis of their force field results.[15] Kramer *et al.* concluded that the strong dependence of ΔU_{trans} on the density as predicted by the KFBS potential is due to an artifact in the C/r^6 term (see above).[5] Johnson *et al.* measured enthalpies for seven silicates. Those data suggested a linear relation between ΔU_{trans} and the density of silicates.[44] Recently Petrovic *et al.*[9] measured the ΔH_{trans} for six silica polymorphs. Those data show, at most, a weak correlation between the density and ΔU_{trans} for silica polymorphs (see Fig. 6). Our calculations show the following. Figure 6 shows JC and BJS II results of ΔU_{trans} versus the density for the silicates in Table V. Linear fits on those data, as shown in Fig. 6, reveal that both potentials do not predict a real correlation between ΔU_{trans} and the density for a large number of structures. This is consistent with the recent results of Petrovic *et al.* We therefore conclude that a linear relation between ΔU_{trans} and density is not likely to hold for a large number of silicates.

2. Correlation between the percentage Si-O-Si smaller than or equal to 140° and ΔU_{trans}

Petrovic *et al.*[9] proposed on basis of enthalpy measurements for six silicates that there should exist a linear relationship between the percentage of Si-O-Si bond angles smaller than or equal to 140° in the structure and ΔU_{trans}. To investigate this more thoroughly we have evaluated BJS II and JC predictions for more silicates with narrow Si-O-Si bond angles. Figure 7 shows linear fits on JC and BJS II predictions for ΔU_{trans} versus the above-mentioned percentage. Both potentials predict that this linear relation is not expected to hold when more structures are considered.

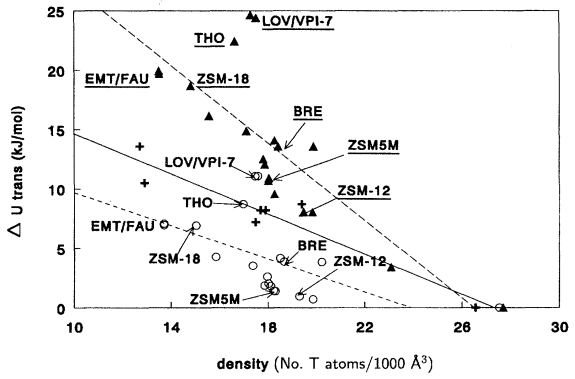

FIG. 6. JC and BJS II predictions of ΔU_{trans} vs density for the silicates in Table V, compared with experiment. Solid triangles and underlined abbreviations depict JC predictions. Open circles and remaining abbreviations depict BJS II predictions. Crosses depict data of Petrovic *et al.*, see Table IV. The abbreviations depict silicates containing Si-O-Si bond angles smaller than or equal to 140°. The lower line represents a linear fit on BJS II predictions, rms error of this fit is 2.75 kJ/mol. The middle line represents a linear fit on data of Petrovic *et al.*, rms error of this fit is 1.20 kJ/mol. The upper line represents a linear fit on JC predictions, rms error of this fit is 3.95 kJ/mol. ZSM-5-m denotes monoclinic ZSM-5.

3. Relation between structure and ΔU_{trans} for low-density silicates

Petrovic *et al.* have hypothesized that pure-silica materials with large pores (i.e., in the low-density region) are not destabilized by their large cages but by the presence of small Si-O-Si bond angles in the structure, which is then the reason why they are so difficult to synthesize. This hypothesis is based on enthalpies of three low-density silicates. To test this

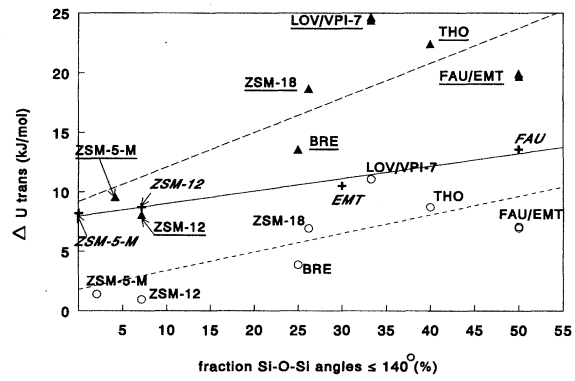

FIG. 7. ΔU_{trans} vs fraction of angles smaller than or equal to 140° as predicted by the BJS II and JC potentials for the systems mentioned in Table V which contain small angles, compared with experimental values of those systems in Table IV which contain small angles. Abbreviations in slanted type depict experiment, remaining abbreviations are as in Fig. 6. The lower line represents a linear fit on BJS II predictions, rms error of this fit is 2.63 kJ/mol. The middle line represents a linear fit on experimental values, rms error of this fit is 0.38 kJ/mol. The upper line represents a linear fit on JC predictions, rms error of this fit is 3.82 kJ/mol.

hypothesis, we have considered BJS II and JC predictions for a larger number of low-density silicates. The BJS II and JC predictions on hexagonal faujasite, cubic faujasite, ZSM-18, VPI-7, lovdarite, and thomsonite, which are all in the lower-density region, show that those structures are less stable than the remaining structures, see Figs. 6 and 7. Figure 7 shows that those structures contain a significant percentage of angles smaller than or equal to 140°. Tables II and III show that those structures contain, except the small Si-O-Si bond angles, no *other* anomalous angles and distances, which might be responsible for instability. Thus the instability of those structures must be caused by small Si-O-Si bond angles, which supports the hypothesis of Petrovic *et al.* We note in passing that this hypothesis also explains why cubic faujasite is more unstable as ZSM-18, something which could not be explained by the presence of three-rings in the structure.[3,39,40,45] Furthermore, we expect that this hypothesis does not hold for higher-density zeolites because Figs. 6 and 7 show that in the higher-density region, silicates with a significant percentage of Si-O-Si bond angles smaller than or equal to 140°, are not necessarily less stable than other systems.

IV. CONCLUSIONS

Our main result is that we have developed a new *ab initio* based shell-model potential (BJS II) which is equally accurate as the JC potential on structure predictions. Inclusion of structure data on α quartz in the BJS II potential improved all structure predictions studied. The predictions of those potentials for well-defined structures are much closer to the experiment than the BJS I, TTA, and KFBS potential. The BJS II and JC results further indicate that the Si-O distances and O-Si-O angles as measured for ZSM-11 and ZSM-12 may not be accurate. The fact that the BJS II and the JC potentials have been derived in completely different manners (*ab initio* versus semiempirical), and yet yield such similar results for structures, implies that these potentials should be very reliable on the predictions of those properties. The accurate structure predictions of the JC potential combined with reasonable stability predictions, makes this potential suitable for the exploration of hypothetical structures and the study of structure-stability relationships. To a lesser extent this also holds for the BJS II potential which gives accurate structure predictions, but less accurate predictions for the relative stabilities of silicates. The above relationships cannot be studied with the KFBS and TTA potential, because they predict both the structure and relative stability of silicates less accurately.

Furthermore, the higher accuracy of the BJS I, BJS II, and JC stability predictions, compared to those of the KFBS and TTA potentials, indicates that a shell model might be mandatory for a good prediction of the stability. With respect to the structure-stability relationships we conclude the following. *Both* the JC and BJS II potentials predict that there exists no linear relation between ΔU_{trans} and the density of silicates. Those potentials also consistently predict that low-density silicates are destabilized by their narrow Si-O-Si bond angles. This supports the hypothesis of Petrovic *et al.* that pure-silica large-pore (i.e., low-density) materials are destabilized by small Si-O-Si bond angles in the structure. This makes them more difficult to synthesize than materials containing Be, B, and Zn, because the presence of the latter elements favors smaller T-O-T bond angles,[9] which, as we have shown, is due to the T-O distances in those structures, which are much larger than in the all-silica structures. However, according to the JC and BJS II results, a linear relation between the percentage of angles smaller than or equal 140° and ΔU_{trans}, as proposed by Petrovic *et al.*,[9] is not likely to exist for a large number of silicates.

ACKNOWLEDGMENTS

This work was supported by the Netherlands Foundation for Chemical Research (SON) with financial aid from the Netherlands Organization of Pure and Applied Research (NWO).

[1] *Solid State Chemistry*, edited by A. K. Cheetham and P. Day (Oxford University, Press, New York, 1990), Vol. 2.

[2] P. A. Jacobs and J. A. Martens, *Synthesis of High Silica Alumino Silicate Zeolites* (Elsevier, Amsterdam, 1987).

[3] R. A. van Santen, G. Ooms, J. J. den Ouden, B. W. H. van Beest, and M. F. M. Post, ACS Symp. Series **398**, 617 (1989).

[4] R. A. van Santen, B. W. H. van Beest, and A. J. M. de Man, *Guidelines for Mastering the Properties of Molecular Sieves*, edited by D. Bartomeuf *et al.* (Plenum, New York, 1990).

[5] G. J. Kramer, A. J. M. de Man, and R. A. van Santen, J. Am. Chem. Soc. **113**, 6435 (1991).

[6] J. B. Nicolas, A. J. Hopfinger, F. R. Trouw, and L. E. Iton, J. Am. Chem. Soc. **113**, 4792 (1991).

[7] R. A. Jackson and C. R. A. Catlow, Mol. Simul. **1**, 207 (1988).

[8] N. J. Henson, A. K. Cheetham, and J. D. Gale, Chem. Mater. **6**, 1647 (1994).

[9] I. Petrovic, A. Navrotsky, M. E. Davis, and S. I. Zones, Chem. Mater. **5**, 1805 (1993).

[10] A. J. M. de Man, H. K. Küppers, and R. A. van Santen, J. Phys. Chem. **96**, 2092 (1992).

[11] K. de Boer, A. P. J. Jansen, and R. A. van Santen, Chem. Phys. Lett. **223**, 46 (1994).

[12] K. de Boer, A. P. J. Jansen, and R. A. van Santen (unpublished).

[13] G. J. Kramer, N. P. Farragher, B. W. H. van Beest, and R. A. van Santen, Phys. Rev. B **43**, 5068 (1991).

[14] S. Tsuneyuki, M. Tsukada, H. Aoki, and Y. Matsui, Phys. Rev. Lett. **61**, 869 (1988).

[15] E. de Vos Burchard, V. A. Verheij, H. van Bekkum, and B. van de Graaf, Zeolites **12**, 183 (1992).

[16] G. A. Lager, J. D. Jorgensen, and F. J. Rotella, J. Appl. Phys. **53**, 6751 (1982).

[17] K. L. Geisinger, M. A. Spackman, and G. V. Gibbs, J. Phys. Chem. **91**, 3237 (1987).

[18] W. Sinclair and A. E. Ringwood, Nature **272**, 714 (1978).

[19] C. A. Fyfe, H. Gies, G. T. Kokotailo, C. Pasztor, H. Strobl, and D. E. Cox, J. Am. Chem. Soc. **111**, 2470 (1989).

[20] C. A. Fyfe, H. Gies, G. T. Kokotailo, B. Marler, and D. E. Cox, J. Phys. Chem. **94**, 3718 (1990).
[21] S. L. Lawton and W. J. Rohrbaugh, Science **247**, 1319 (1990).
[22] J. A. Hriljac, M. M. Eddy, A. K. Cheetham, J. A. Donahue, and G. J. Ray, J. Solid State Chem. **106**, 66 (1993).
[23] H. van Koningsveld, J. C. Jansen, and H. van Bekkum, Zeolites **10**, 235 (1990).
[24] R. Bialeck, W. M. Meier, M. E. Davis, and M. J. Annen, Zeolites **111**, 438 (1991).
[25] B. Marler, Zeolites **7**, 393 (1987).
[26] K. A. van Gnechten and W. J. Mortier, Zeolites **8**, 273 (1988).
[27] J. V. Smith, F. Rinaldi, and L. S. Dent Glasser, Acta Crystallogr. **16**, 45 (1963).
[28] S. Merlino, Eur. J. Miner. **2**, 809 (1990).
[29] M. J. Annen, M. E. Davis, J. B. Higgins, and J. L. Schlenker, J. Chem. Soc., Chem. Commun. 1175 (1991).
[30] J. M. Newsam, M. M. Treacy, D. E. W. Vaughan, K. G. Strohmaier, and W. J. Mortier, J. Chem. Soc., Chem. Commun. 493 (1989).
[31] I. Hassan and H. D. Grundy, Acta Crystallogr. B **40**, 6 (1984).
[32] W. M. Meier, Z. Kristallogr. **115**, 439 (1961).
[33] C. R. A. Catlow and W. C. Mackrodt, *Computer Simulations in Physics,* Lecture Notes in Physics (Springer, Vienna, 1982); C. R. A. Catlow, M. Doverty, G. D. Price, M. J. Sanders, and S. C. Parker, Mater. Sci. Forum **7**, 163 (1986); M. Leslie, THBREL, Science and Engineering Research Council, Daresbury Laboratory, U.K.
[34] C. R. A. Catlow and M. J. Norgett (private communication).
[35] G. Dolling, *Calculations of Phonon Frequencies in Methods in Computational Physics* (Academic, New York, 1976), Vol. 15; M. Leslie, THBPHON, Science and Engineering Research Council, Daresbury Laboratory, U.K.
[36] K. de Boer, A. P. J. Jansen, R. A. van Santen, and S. C. Parker (unpublished).
[37] A. J. M. de Man, W. P. J. H. Jacobs, J. P. Gilson, and R. A. van Santen, Zeolites **12**, 826 (1992).
[38] A. Kirfel, G. Will, and J. Arndt, Z. Kristallogr. **149**, 315 (1979).
[39] J. D. Gale, C. R. A. Catlow, and W. C. Mackrodt, Modeling Simul. Mater. Sci. Eng. **1**, 73 (1992).
[40] A. J. M. de Man, S. Ueda, M. J. Annen, M. E. Davis, and R. A. van Santen, Zeolites **12**, 789 (1992).
[41] S. C. Parker and G. D. Price, Adv. Solid State Chem. **1**, 295 (1989).
[42] K. Kihara, Eur. J. Miner. **2**, 63 (1990).
[43] J. J. Pluth, J. V. Smit, and J. Faber, Jr., J. Appl. Phys. **57**, 1045 (1985).
[44] G. K. Johnson, I. R. Tasker, and D. A. Howell, J. Chem. Thermodynam. **19**, 617 (1987).
[45] J. D. Gale and A. K. Cheetham, Zeolites **12**, 674 (1992).